



# Sol-gel synthesis of gelatin-zirconium(IV) tungstophosphate nanocomposite ion exchanger and application for the estimation of Cd(II) ions

Manita Thakur<sup>1</sup> · Deepak Pathania<sup>2</sup>

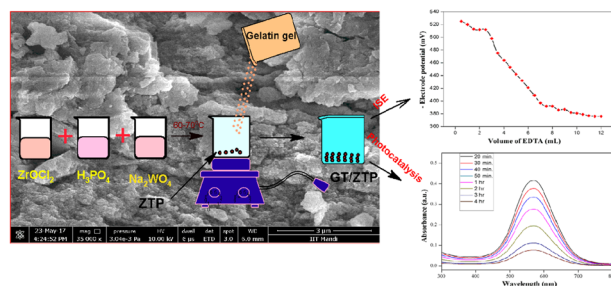
Received: 8 October 2018 / Accepted: 3 January 2019 / Published online: 12 January 2019  
© Springer Science+Business Media, LLC, part of Springer Nature 2019

## Abstract

Gelatin-Zr(IV) tungstophosphate (GT/ZTP) nanocomposite ion exchanger was synthesised using simple sol-gel method at pH 0–1. GT/ZTP nanocomposite shows greater value of IEC (0.80 meq/g) as compared to Zr(IV) tungstophosphate (0.32 meq/g). TEM results confirmed the nano size of composite material. Distribution coefficient studies illustrates that the GT/ZTP have higher distribution coefficient values for Cd(II) instead of others. Binary separations of metal ion pairs including Cd(II)–Al(III), Cd(II)–Ni(II), Pb(II)–Mg(II), Mg(II)–Zn(II), Pb(II)–Cu(II), Co(II)–Cu(II), Al(III)–Co(II) and Ni(II)–Zn(II) were attempted using GT/ZTP nanocomposite column. The photocatalytic studies showed that 84.61% MV was degraded within 4 h of solar illumination. The kinetics of photocatalytic degradation for methyl violet (MV) was studied by pseudo-first-order kinetic model with higher  $R^2 = 0.998$ . GT/ZTP nanocomposite was exploited for the erection of ion selective membrane electrode to detect Cd(II) in the water system. The electrode possessed wide concentration range, pH range and quick response time.

## Graphical Abstract

Sol-gel synthesis of GT/ZTP nanocomposite for the detection of cadmium ions and enhanced photocatalytic studies for the removal of dye from water system.



## Highlights

- A heterogeneous ion-selective membrane electrode was fabricated to detect Cd(II) using GT/ZTP nanocomposite.
- GT/ZTP nanocomposite was highly selective for Cd<sup>2+</sup> ions.
- Some binary separations of different metal ions were accomplished onto GT/ZTP column.
- GT/ZTP was used as photocatalyst for the degradation of MV under solar illumination.

**Keywords** Nanocomposite · Gelatin · Heavy metals · Methyl violet · Electrode · Zirconium tungstophosphate

✉ Deepak Pathania  
dpathania74@gmail.com

<sup>1</sup> Department of Chemistry, Maharishi Markandeshwar University,  
Solani, Himachal Pradesh 173212, India

<sup>2</sup> Department of Environmental Sciences, Central University of  
Jammu, Bagla (Rahya-Suchani), Distt. Samba, Jammu & Kashmir  
181143, India

## 1 Introduction

The exploitation of natural resources cause serious environmental issues including air, soil and water pollution [1]. Degradation of water sources by textile, manufacturing, plastics, fuel, fishing, mining and agriculture processes is a severe universal issue [2, 3]. The industrial waste that has been discharged into water system is harmful to living organisms. The industrial waste generally contains heavy metals, antibiotics, dyes, pesticides and phenols [4].

The heavy metals like chromium, lead, cadmium, zinc, nickel, mercury, copper, aluminium and arsenic are major inorganic pollutants [5, 6]. These are exceedingly noxious, non-biodegradable and bio-accumulate [7]. The high intake of heavy metals posed harmful effects to humans, such as emphysema, hypertension, renal damage and skeletal malformation [8, 9]. Dyes are toxic contaminants frequently employed in industrial activities, such as textile, paper, leather, etc. [10]. The intake of dyes imparts harmful effects on human body including contact dermatitis, respiratory diseases, irritation in eyes and mucous membrane [11, 12]. Dyes are highly toxic, carcinogenic and mutagenic to living persons [13–15].

Dyes and heavy metals are major pollutants that cause severe toxicity and are highly accumulative in the environment [16]. Therefore, exploitation of these pollutants from industrial wastewater is essential to control environmental pollution [17, 18]. The techniques such as adsorption, precipitation, flotation, membrane, electrochemical treatment and ion exchange have been explored to target different pollutants from water system [19]. But among all these, ion exchange process is of great significance. It is because of its simplicity, low cost, easy operation and effectiveness [20, 21].

Now, researchers have emphasized on prepartion of composite on exchangers with superior properties, such as large ion exchange capacity, chemical, thermal, radiation and mechanical stability over inorganic and organic ion exchangers [22, 23]. At nano range, composite ion exchangers exhibit exchange of ions between the interfaces of phases and enhanced the properties of materials for environmental remediation [24]. Now, polymer-based composite ion exchangers are of great interest because of their unique characteristics, such as bio-degradability and low cost [25, 26]. The polymeric part of composite ion exchanger enhanced the surface area and enhanced the properties of ion exchanger [27].

Gelatin is a colourless, translucent, brittle, flavourless and biodegradable protein formed by acidic or basic hydrolysis of collagen [28, 29]. It is employed as gelling agent in ice creams, yoghurt, food, gummy candy, photography, vitamin capsules, cosmetics and pharmaceutical drugs [30, 31]. Gelatin is made up of peptides and proteins

and extracted from the skin, bones, connective tissues of animals [32, 33]. It dissolves in hot water to form a gel on cooling [34] and used in tissue engineering, wound dressing, gene therapy and drug delivery [35, 36].

The present study shows the synthesis of gelatin–zirconium(IV) tungstophosphate (GT/ZTP) nanocomposite ion exchanger. GT/ZTP was characterised using FTIR, XRD, TGA, SEM and TEM techniques. Physicochemical properties of nanocomposite were also studied in detail. GT/ZTP was used for the binary separations of different metal ion pairs. Photocatalytic activity of GT/ZTP was also studied for the photocatalytic removal of MV. The ion selective electrode was designed using nanocomposite for the detection of Cd(II) ions.

## 2 Experimental

### 2.1 Reagents and instruments

The reagents zirconium(IV) oxychloride, orthophosphoric acid, sodium tungstate were obtained from Loba Cheme Pvt. Ltd. Gelatin, cadmium nitrate, copper nitrate, aluminium nitrate, nickel nitrate, magnesium nitrate, lead nitrate, cobalt nitrate, polyvinyl chloride (PVC) and tetrahydrofuran (THF) were procured from CDH, India. All the reagents and chemicals were of analytical grade and used without any treatment. The instruments used were pH meter (Elico LI10 model, India), muffle furnace (MSW-275, India), magnetic stirrer and digital potentiometer (Electronics, India). The nanocomposite was characterised by Fourier transform infra-red spectrometer (Perkin Spectrum-400), thermogravimetric analysis (Shimadzu thermal analyser TGA50 model-Japan), X-ray diffractometer (X'pert Pro Analytical, Netherlands), scanning electron microscope (Nova nano SEM, 450) and transmission electron microscope (Hitachi H7500 model, Germany).

### 2.2 Synthesis of ZTP

ZTP was prepared by mixing 0.1 M zirconium oxychloride, 0.1 M orthophosphoric acid and 0.1 M sodium tungstate in a volume ratio 2:1:1 with continuous stirring at 60 °C. The pH of above mixture was kept at 0–1 using 0.1 N nitric acid and stirred for 2 h. Then the resulting mixture was filtered and washed several times with double-distilled water and dried at 60 °C for 24 h.

### 2.3 Synthesis of GT/ZTP nanocomposite ion exchanger

GT/ZTP was prepared using sol–gel method [37, 38]. 0.1 M  $ZrOCl_2$ , 0.1 M  $H_3PO_4$  and 0.1 M  $Na_2WO_4$  were mixed at

**Table 1** Conditions for the preparation of various samples of GT/ZTP nanocomposite ion exchanger

Sl. no.	A (mol L <sup>-1</sup> )	B (mol L <sup>-1</sup> )	C (mol L <sup>-1</sup> )	D (%)	Mixing ratio	Temp. (°C)	Appearance	Ion exchange capacity (meq/g)	Yield (g)
S-1	0.1	0.1	0.1	–	2:1:1	60	White	0.33	1.08
S-2	0.1	0.1	0.1	0.2	2:1:1	60	White	0.36	1.12
S-3	0.1	0.1	0.1	0.4	2:1:1	60	Light yellow	0.39	1.20
S-4	0.1	0.1	0.1	0.6	2:1:1	60	Yellow	0.42	1.55
S-5	0.1	0.1	0.1	0.8	2:1:1	60	Yellow	0.45	1.60
S-6	0.1	0.1	0.1	1.0	2:1:1	60	Yellow	0.58	1.63
<b>S-7</b>	<b>0.1</b>	<b>0.1</b>	<b>0.1</b>	<b>1.2</b>	<b>2:1:1</b>	<b>60</b>	<b>Yellow</b>	<b>0.80</b>	<b>1.77</b>
S-8	0.1	0.1	0.1	1.4	2:1:1	60	Yellow	0.72	1.79
S-9	0.1	0.1	0.1	1.6	2:1:1	60	Yellow	0.63	1.82
S-10	0.1	0.1	0.1	1.8	2:1:1	60	Yellow	0.61	1.88

A: Zirconium oxychloride; B: Orthophosphoric acid; C: Sodium tungstate; D: Gelatin

the ratio of 2:1:1 with constant stirring. The pH of solution was kept between 0 and 1 by adding 0.1 M HNO<sub>3</sub>. Then, 1.2% of gelatin gel was added to hot water and poured to the above solution with continuous stirring. The resultant mixture was stirred for 2 h and the obtained precipitates were kept for digestion for 24 h. Finally, the precipitates were filtered and washed with double-distilled water 2–3 times. The precipitates of GT/ZTP were dehydrated at 50 °C and transformed into H<sup>+</sup> by keeping it in 0.1 N HNO<sub>3</sub> for 24 h. The precipitates were separated and washed with distilled water to remove the excess of acid. In the same method, different samples of GT/ZTP nanocomposite have been prepared by varying the percentage of gelatin as summarised in Table 1. The sample S-6 with higher ion exchange capacity was considered for detailed study.

## 2.4 Physicochemical properties

### 2.4.1 Ion exchange capacity

The ion exchange capacity of the GT/ZTP nanocomposite was determined by column method. 1.0 g of ion exchanger was placed in a glass column and packed with glass wool. Firstly, the column was washed with double-distilled water and then passed through 0.1 M solution of the sodium chloride at a flow rate of 20–25 drops/min. The collected effluent was titrated with NaOH using phenolphthalein indicator. The ion exchange capacity was calculated by the formula as discussed in literature [6].

### 2.4.2 Effect of eluent concentration and elution behaviour

In this, 250 mL of sodium nitrate (0.3, 0.6, 0.9, 1.2, 1.5 and 1.8 M) was used to elute H<sup>+</sup> ions from GT/ZTP column. The eluent of different concentrations passed through column with 1.0 g of ion exchange material (in H<sup>+</sup> form) at a flow rate of 20–25 drops/min. The collected solution was

titrated with 0.1 M sodium hydroxide solution. The ion exchange capacity at each concentration was calculated using the formula as discussed above in the section “Ion exchange capacity”. The elution behaviour was determined using 1.0 g of GT/ZTP in H<sup>+</sup> form and eluted with 1.2 M NaNO<sub>3</sub> solution. The effluent was collected in 10 mL fractions at a flow rate of 20–25 drops/min and titrated with NaOH [6].

### 2.4.3 pH titration

pH titration studies of ion exchanger were examined by Topp and Pepper method as discussed in literature [9].

### 2.4.4 Thermal studies

To examine the thermal stability of GT/ZTP, 1.0 g of nanocomposite was heated over a wide temperature range (100–600 °C) in a muffle furnace for 1 h. Then, after cooling, ion exchange capacity of nanocomposite was calculated by column method as discussed above.

### 2.4.5 Distribution coefficients

The distribution coefficients of eight metals onto GT/ZTP were determined by batch method as discussed in literature. Two hundred micrograms of ion exchanger in H<sup>+</sup> form was added into 20 mL of different metal nitrates taken in Erlenmeyer flask. The mixture was kept for 24 h with continuous stirring to achieve the equilibrium. The concentrations of different metal ion solutions were examined by titrating against EDTA [6, 9].

## 2.5 Binary separations

Various quantitative binary separations of metal ions were attained on GT/ZTP column. One gram of ion exchanger

was placed in a column fitted with glass wool and washed with double-distilled water. The mixture of two metal ions was passed through the column at a flow rate of 20–25 drops/min. To remove the metal ions that are adhered to the column, it is washed with distilled water. The adsorbed metal ions on GT/ZTP were eluted with different concentrations of solvent. The effluents were collected in 10 mL fractions and titrated with EDTA [37].

## 2.6 Photocatalytic activity

The photocatalytic activity of GT/ZTP was examined for the photocatalytic removal of methyl violet (MV) using batch method. Hundred micrograms of nanocomposite was added to the  $1.5 \times 10^{-5}$  M dye solution to form slurry. The slurry was placed in dark with constant stirring for 1 h to maintain adsorption–desorption equilibrium. Then, the slurry was exposed to sunlight for further photocatalysis with constant stirring. Five microliters of dye solution was withdrawn and centrifuged at different time intervals. The concentration of MV was determined by UV–vis spectrophotometer at 564 nm. The percent degradation of dye was calculated by the equation as reported in literature [38].

## 2.7 Preparation of GT/ZTP nanocomposite membrane

The ion exchange membranes of different thicknesses was prepared by using nanocomposite as described in literature in detail [39, 40]. Three membranes of different thickness were obtained as shown in Table 5. The membranes were cut into round shape and fixed at the end of glass tube with PVC [41].

### 2.7.1 Characterisation of membrane

Some parameters of membranes, such as total wet weight, porosity, thickness and swelling are discussed as given below

#### 2.7.2 % total wet weight

The membranes were dipped in double-distilled water and blotted quickly with Whatman filter paper to remove the surface moisture. Then, membranes were weighed and dried for 24 h. The total wet weight was calculated using formula as discussed earlier [42].

#### 2.7.3 Porosity

The porosity of membranes was determined by using equation as discussed in literature [43].

### 2.7.4 Thickness and swelling

Thickness of the membranes was determined using screw gauze. The swelling of membranes was measured by taking the difference between average thickness of the membrane when equilibrated in  $1 \text{ mol L}^{-1}$  NaCl for 24 h and weight of dry membrane.

## 2.8 Fabrication of ion-selective membrane electrode

The membrane (M-2) of 0.49 mm thickness was cut into round shape and fixed at the lower end of glass tube with PVC. It was dried in air for 24 h and filled with 0.1 M cadmium nitrate. A saturated calomel electrode (SCE) was used as an internal reference electrode and inserted into the metal solution. Another SCE was used as an external reference electrode [44]. Various parameters of electrode, such as electrode response curve, working pH range, potentiometer titration and response time were determined as follows:

### 2.8.1 Electrode response

The electrode response of GT/ZTP membrane electrode was determined by the method as discussed earlier. In this, Cd ( $\text{NO}_3$ )<sub>2</sub> solutions of different concentrations that ranged from  $1 \times 10^{-1}$  to  $1 \times 10^{-10}$  were prepared. Firstly, the electrode was conditioned by dipping in  $0.1 \text{ mol L}^{-1}$  Cd ( $\text{NO}_3$ )<sub>2</sub> solution for 5–7 days and the potentials were recorded at different concentrations. Then, the values of potentials were plotted against selected concentration of the ions.

### 2.8.2 Effect of pH

In this, pH solutions at constant ion concentration range from 1 to 12 were prepared and electrode potential was recorded at each pH. The value of electrode potential was recorded and plotted opposite to pH values.

### 2.8.3 The response time

The membrane electrode was first transferred into  $1 \times 10^{-3} \text{ mol L}^{-1}$  of Cd( $\text{NO}_3$ )<sub>2</sub> solution for 10 s and then shifted to 10-fold higher concentration ( $1 \times 10^{-2} \text{ mol L}^{-1}$ ) solution with continuous stirring. Further, the electrode potential was seen in both the solutions and graph was plotted between potentials versus time.

### 2.8.4 Potentiometric titration

GT/ZTP membrane electrode was used as an indicator electrode in potentiometric titration. Ten milliliters of  $1 \times$

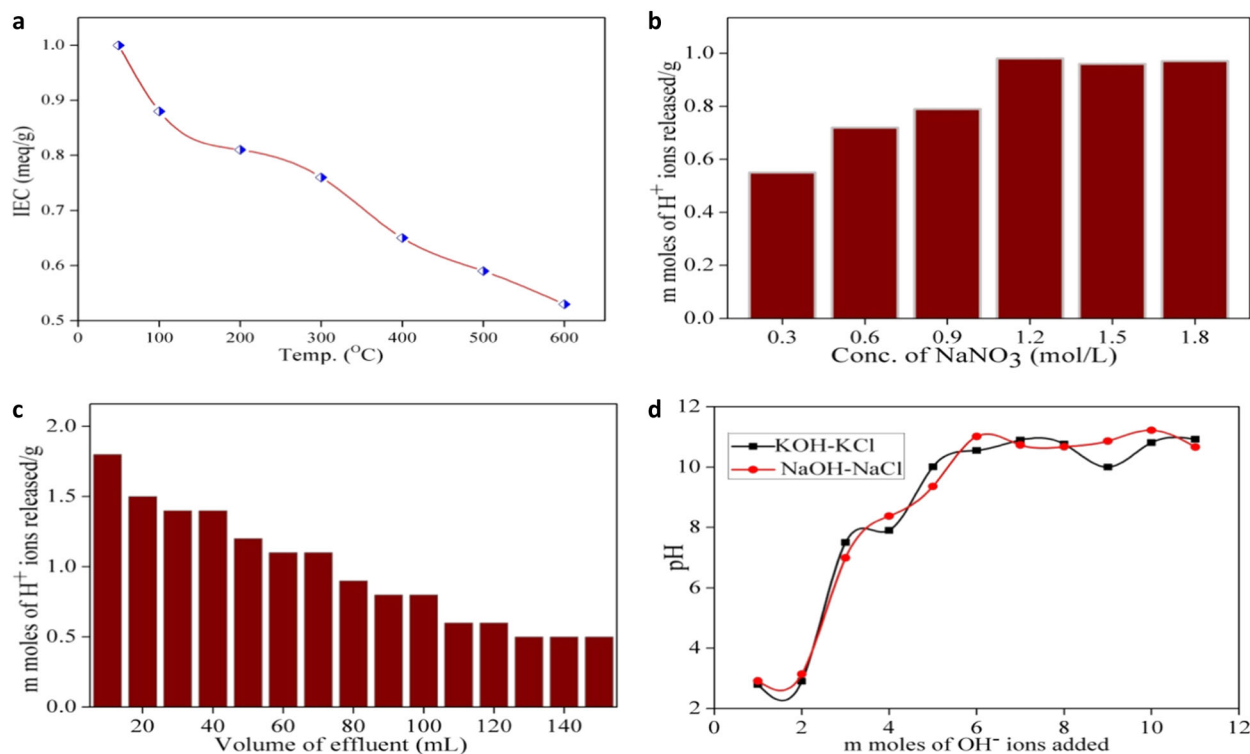


**Fig. 1** **a** Effect of temperature on ion exchange capacity. **b** Effect of eluent concentration. **c** Elution behaviour. **d** pH titration curve of GT/ZTP nanocomposite ion exchanger

$10^{-3} \text{ mol L}^{-1} \text{ Cd(NO}_3)_2$  solution was taken in a 50.0 mL beaker and titrated with  $1 \times 10^{-2} \text{ mol L}^{-1}$  EDTA. The values of electrode potential were drawn opposite to the volume used for EDTA.

### 3 Results and discussion

Ten different samples of gelatin–Zr(IV) tungstophosphate nanocomposite ion exchanger were synthesised using sol-gel method [45]. Sample S-7 with highest ion exchange capacity was considered for detail study. GT/ZTP shows greater ion exchange capacity of 0.80 meq/g than the inorganic counterpart Zr(IV) tungstophosphate, i.e. 0.33 meq/g. It happens by the incorporation of gelatin into ZTP matrix, which introduces large surface area for multiple active donor sites [46]. The fibrous nature provides greater mechanical strength which reduced the leaching of nanocomposite from column [47].

The effect of temperature change on the ion exchange capacity of GT/ZTP was examined as shown in Fig. 1a and Table 2. The ion exchange capacity of material was retained up to 300 °C due to the attachment of organic part. Further, decrease in the ion exchange capacity after 300 °C results due to the disintegration of material into oxides.

**Table 2** Effect of temperature on the ion exchange capacity of GT/ZTP nanocomposite ion exchanger

Heating temperature (°C)	Appearance of colour	Weight loss (g)	K <sup>+</sup> ion exchange capacity (meq/g)
50	Light yellow	–	0.80
100	Yellow	0.88	0.78
200	White	0.81	0.72
300	White	0.76	0.61
400	White	0.65	0.53
500	Brown	0.59	0.45
600	Brown	0.53	0.39

Figure 1b shows that the ion exchange capacity of nanocomposite was observed maximum at 1.2 M NaNO<sub>3</sub>. The optimum concentration for maximum release of H<sup>+</sup> from column of GT/ZTP nanocomposite was observed to be 1.2 M NaNO<sub>3</sub>. Hence, the extent of elution depends on the concentration of eluent used.

Figure 1c represents the elution behaviour of GT/ZTP nanocomposite ion exchanger. One hundred fifty millilitres of NaNO<sub>3</sub> was sufficient for complete release of H<sup>+</sup> from GT/ZTP. It shows good efficiency of GT/ZTP nanocomposite column.

**Table 3**  $K_d$  values of different metal ions on GT/ZTP nanocomposite column

Sl. no.	Metal ions	$K_d$ (mL/g)	
		Distilled water	0.1 N HNO <sub>3</sub>
1	Cd <sup>2+</sup>	280.0	269.56
2	Ni <sup>2+</sup>	159.52	150.82
3	Al <sup>3+</sup>	131.17	114.56
4	Mg <sup>2+</sup>	94.10	90.67
5	Cu <sup>2+</sup>	82.85	73.54
6	Co <sup>2+</sup>	73.93	67.38
7	Zn <sup>2+</sup>	73.07	63.46
8	Pb <sup>2+</sup>	32.27	25.76

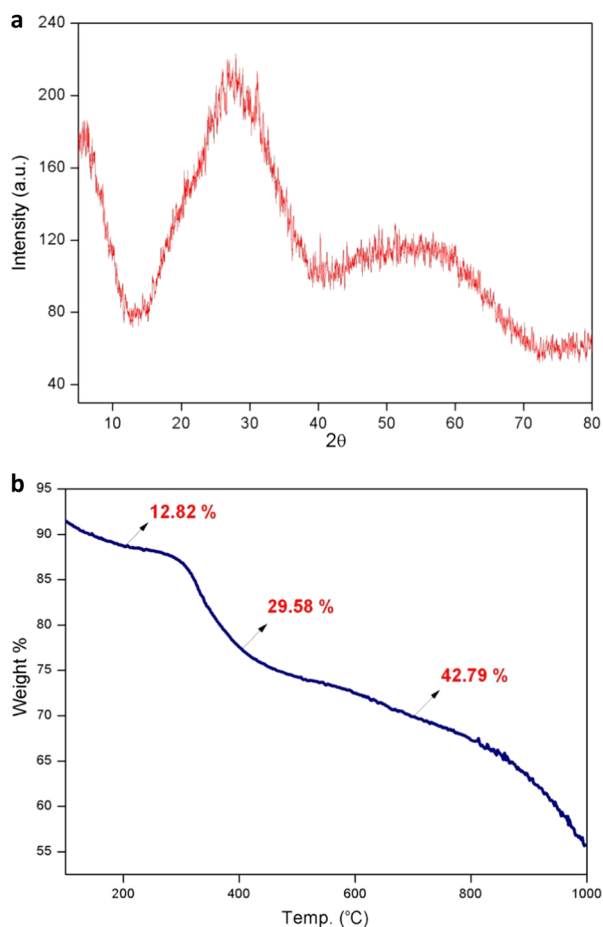
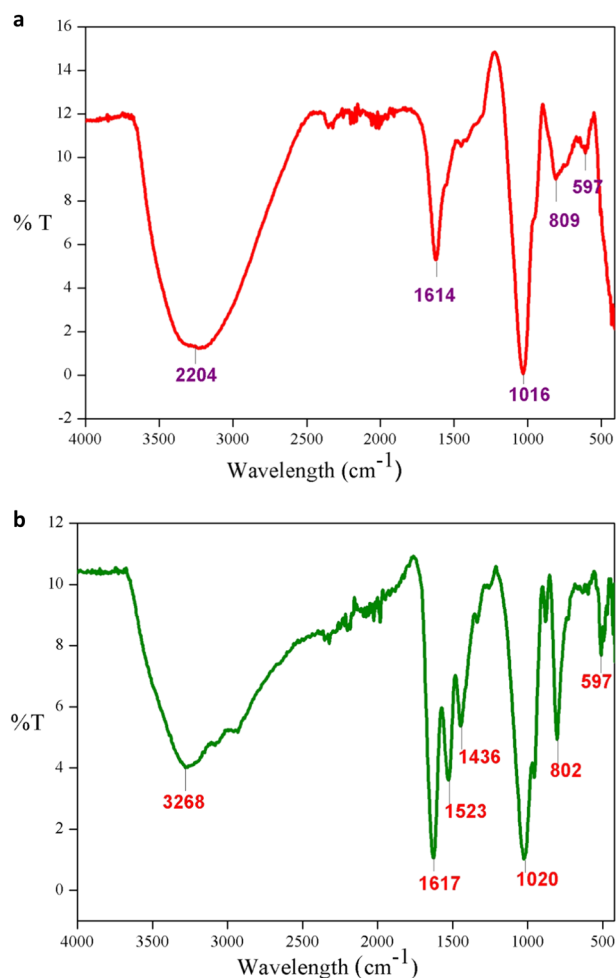
**Fig. 2** **a** XRD spectrum of GT/ZTP nanocomposite. **b** TGA curve of GT/ZTP nanocomposite

Figure 1d shows the pH titration curve of GT/ZTP nanocomposite ion exchanger for NaOH–NaCl and KOH–KCl under equilibrium conditions. The nanocomposite was found bifunctional in nature with two inflection points. The nanocomposite was strong cation exchanger when no OH<sup>-</sup> ions were added to the system. At low pH, weak acidic groups remain undissociated. The addition of NaOH

**Fig. 3** FTIR spectrum of **a** ZTP and **b** GT/ZTP nanocomposite

solution results in dissociation of weak acidic groups and resulting solution gets neutralised. Hence, the process of ion exchange moves towards completion [6].

### 3.1 Distribution studies

Distribution studies of eight metal ions were performed to examine the potentiality of GT/ZTP nanocomposite. Table 3 shows the values of distribution studies for different metal ions. It has been observed that in double-distilled water, Cd (II) was strongly adsorbed with higher  $K_d$  value over other metal ions. It was due to higher concentration of H<sup>+</sup> ions in acidic medium, which reverse the process of adsorption and ion exchange. The order of selectivity of metal ions using GT/ZTP follow the order as Cd<sup>2+</sup> > Ni<sup>2+</sup> > Al<sup>3+</sup> > Mg<sup>2+</sup> > Cu<sup>2+</sup> > Co<sup>2+</sup> > Zn<sup>2+</sup> > Pb<sup>2+</sup>.

### 3.2 Characterisation

Figure 2a shows the XRD spectra of GT/ZTP nanocomposite ion exchanger. The low-intensity peaks were

**Fig. 4** Scanning electron micrographs **a, b** gelatin, **c, d** ZTP and **e, f** GT/ZTP nanocomposite ion exchanger

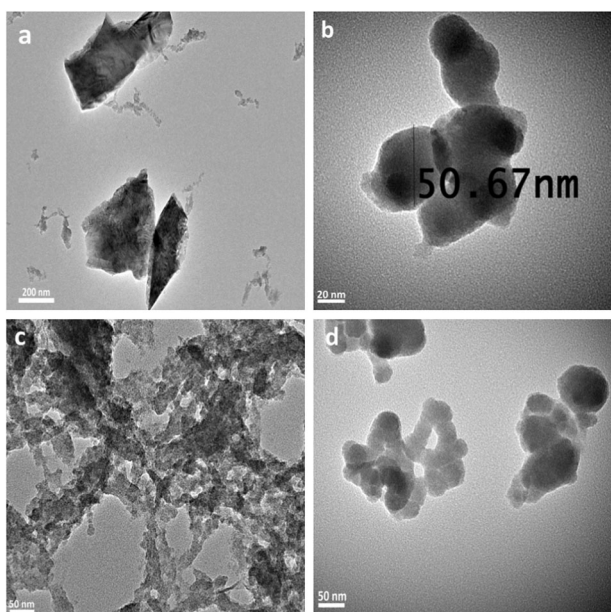
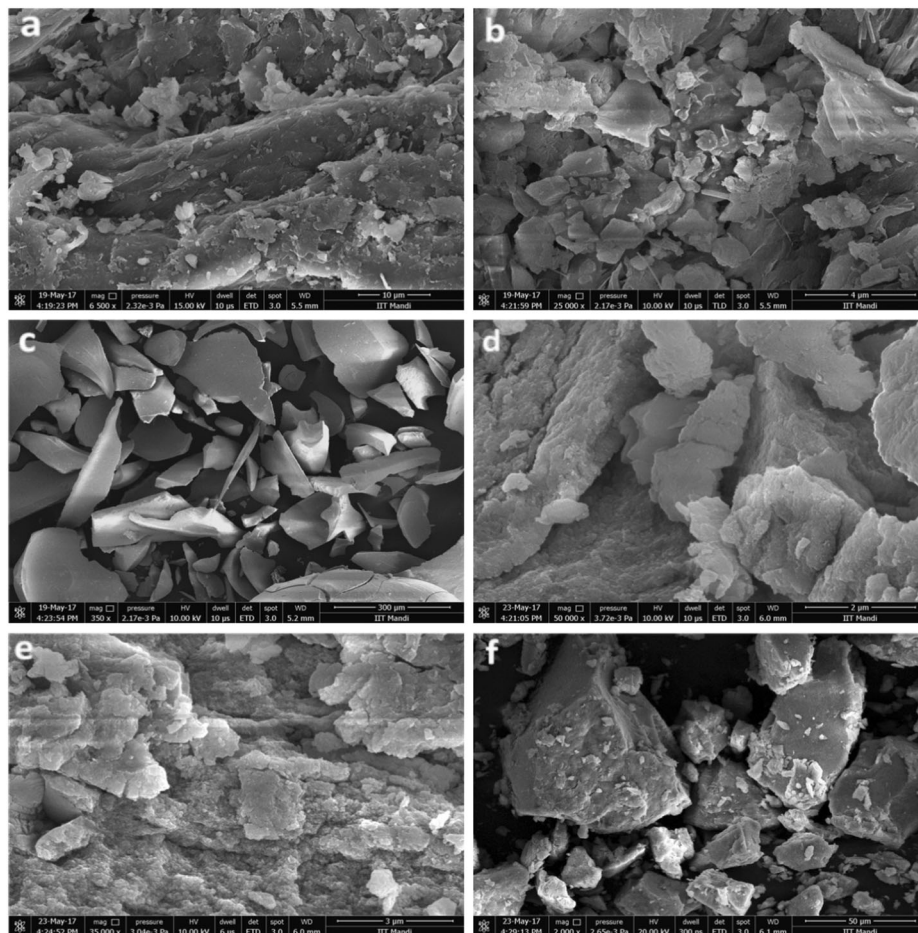


**Fig. 5** **a–d** Transmission electron micrographs of GT/ZTP nanocomposite ion exchanger at different magnifications

**Table 4** Binary separation of metal ions accomplished on the column of GT/ZTP nanocomposite

Binary mix-tures	Amount loaded (mg)	Amount found (mg)	% Recovery	Eluent used	Volume of eluent required for elution of metal ions (mL)
Al <sup>3+</sup>	2.69	1.75	65.19	0.1 N HNO <sub>3</sub>	50
Cd <sup>2+</sup>	11.2	8.43	75.27	0.5 N HNO <sub>3</sub>	70
Ni <sup>2+</sup>	5.86	4.46	76.11	0.1 N HNO <sub>3</sub>	50
Cd <sup>2+</sup>	11.24	10.22	91.00	0.5 N HNO <sub>3</sub>	60
Zn <sup>2+</sup>	6.53	4.64	71.09	0.1 N HNO <sub>3</sub>	50
Mg <sup>2+</sup>	2.43	2.23	92.00	0.5 N HNO <sub>3</sub>	60
Pb <sup>2+</sup>	20.7	11.18	54.05	0.1 N HNO <sub>3</sub>	50
Mg <sup>2+</sup>	2.43	1.77	73.91	0.5 N HNO <sub>3</sub>	70
Pb <sup>2+</sup>	20.7	9.94	48.05	0.1 N HNO <sub>3</sub>	50
Cu <sup>2+</sup>	6.35	4.13	65.05	0.5 N HNO <sub>3</sub>	60
Cu <sup>2+</sup>	6.39	3.26	51.03	0.1 N HNO <sub>3</sub>	50
Co <sup>2+</sup>	5.80	4.59	79.25	0.5 N HNO <sub>3</sub>	70
Co <sup>2+</sup>	5.86	3.88	66.34	0.1 N HNO <sub>3</sub>	50
Al <sup>3+</sup>	2.69	2.59	94.04	0.5 N HNO <sub>3</sub>	60
Zn <sup>2+</sup>	6.53	4.12	65.39	0.1 N HNO <sub>3</sub>	50
Ni <sup>2+</sup>	5.89	5.69	96.20	0.5 N HNO <sub>3</sub>	60

**Fig. 6** Binary separations of  $\text{Cd}^{2+}$ - $\text{Al}^{3+}$ ,  $\text{Cd}^{2+}$ - $\text{Ni}^{2+}$ ,  $\text{Mg}^{2+}$ - $\text{Pb}^{2+}$ ,  $\text{Mg}^{2+}$ - $\text{Zn}^{2+}$ ,  $\text{Cu}^{2+}$ - $\text{Pb}^{2+}$ ,  $\text{Co}^{2+}$ - $\text{Cu}^{2+}$ ,  $\text{Al}^{3+}$ - $\text{Co}^{2+}$  and  $\text{Ni}^{2+}$ - $\text{Zn}^{2+}$  onto GT/ZTP nanocomposite ion exchanger column

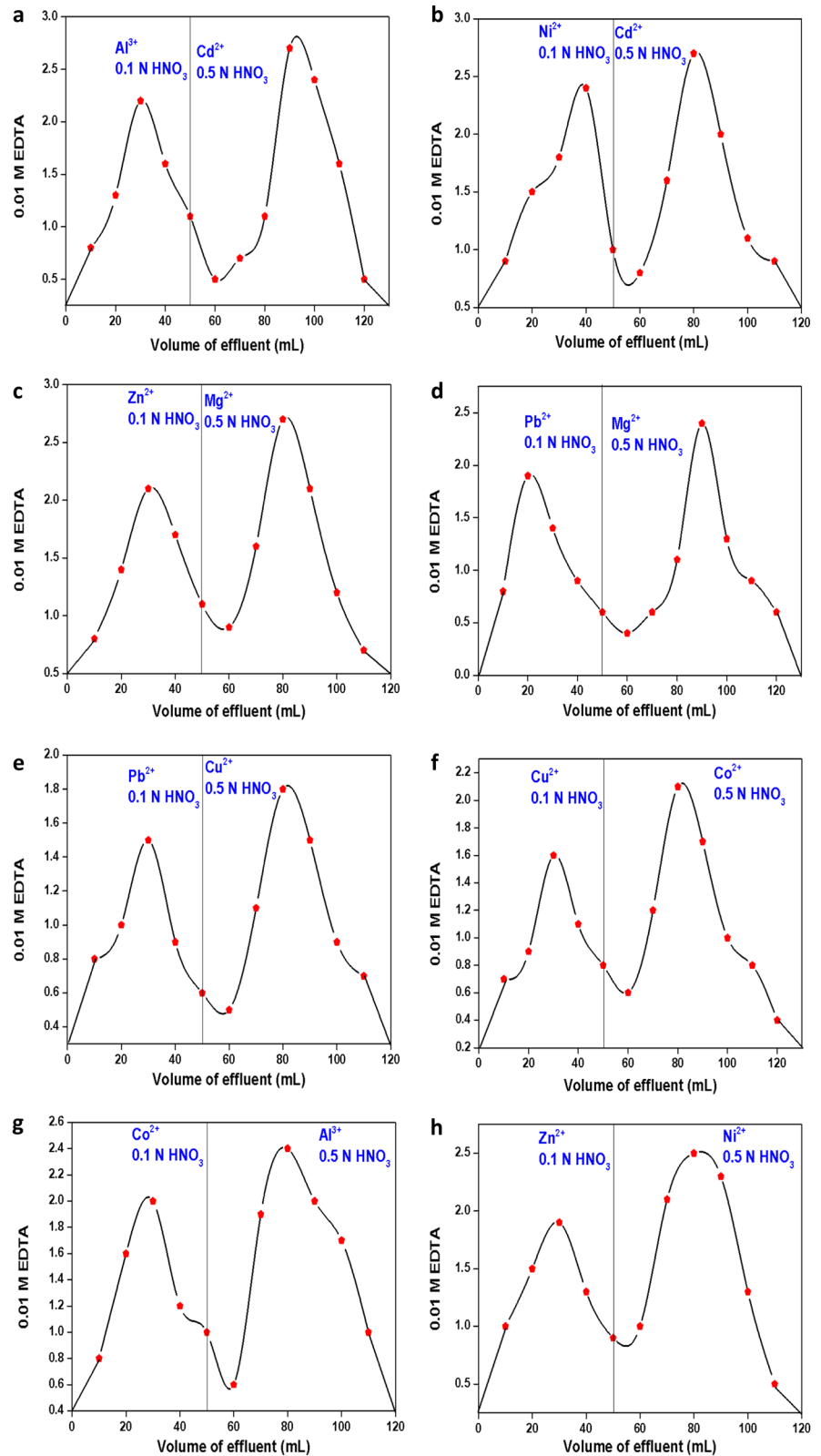
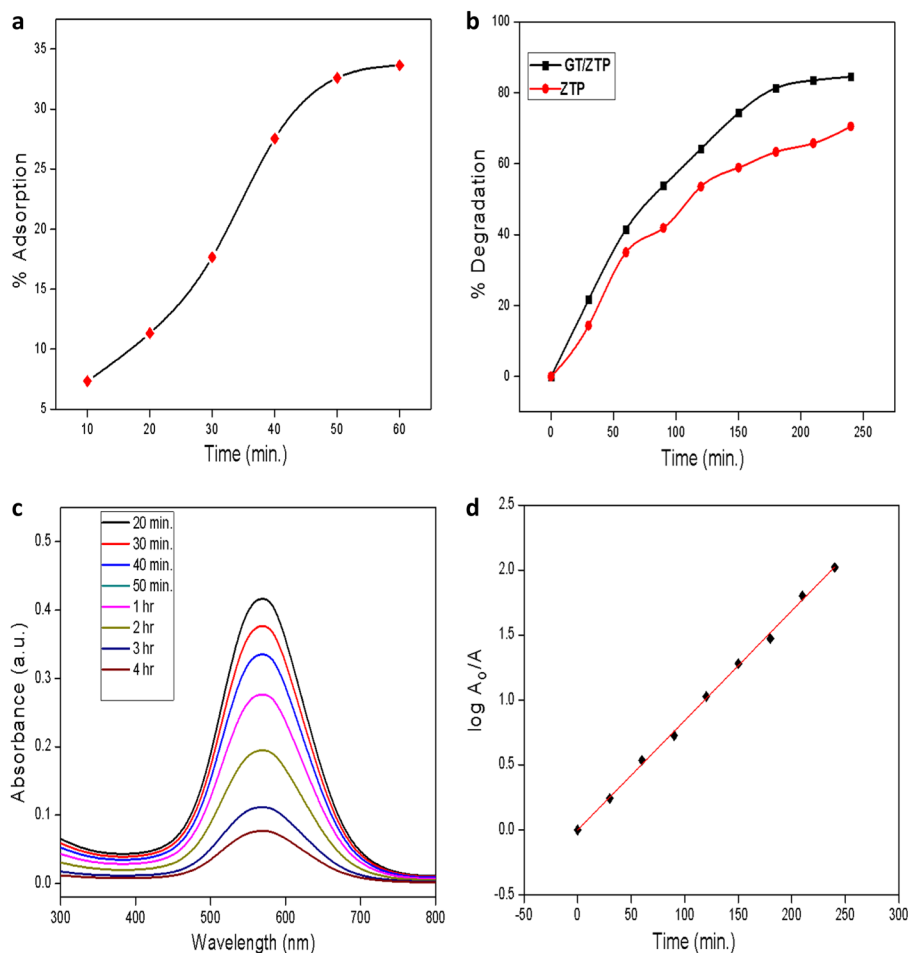




**Fig. 7** **a** Adsorption of MV onto GT/ZTP nanocomposite in dark. **b** Percentage degradation of MV onto ZTP and GT/ZTP nanocomposite in solar illumination. **c** UV–Vis absorption spectrum of MV onto GT/ZTP nanocomposite at different irradiation times. **d** Pseudo-first-order kinetics for photodegradation of MV onto GT/ZTP nanocomposite



recorded in the spectra of composite and confirmed the semi-crystalline nature of GT/ZTP.

Figure 2b shows the TGA curve of GT/ZTP nanocomposite ion exchanger. In this, 12.82% weight loss was recorded up to 200 °C due to the removal of free external water molecules. Further, the 29.58% weight loss was observed from 200 to 400 °C. It was due to the decomposition of organic part. 42.79% weight loss was noticed from 400 to 700 °C due to the condensation of phosphate group to pyrophosphate. Above 700 °C, the weight loss was almost constant due to formation of metal oxides [9].

FTIR spectra of ZTP and GT/ZTP nanocomposite ion exchangers are shown in Fig. 3a, b. A broad peak at 3268 and 1617  $\text{cm}^{-1}$  corresponds to O–H stretching of lattice water and amide bond stretching [48]. The peaks at 1020, 802 and 597  $\text{cm}^{-1}$  were observed due to ionic phosphate stretching, tungstate and metal oxide groups. The additional peaks at 1523 and 1436  $\text{cm}^{-1}$  are attributed to  $\text{COO}^-$  symmetric stretching and  $-\text{CH}_3$  asymmetric bending, confirms the formation of nanocomposite ion exchanger.

Figure 4a, b and c, d shows the scanning electron micrographs of gelatin and ZTP. SEM images of GT/ZTP nanocomposite are shown in Fig. 4e, f. It has been observed that the surface morphology was completely reformed into rough, granular and irregular surface, which indicated the formation of nanocomposite.

Figure 5a–d shows the TEM images of GT/ZTP at different magnifications. TEM images confirmed the particle size of composite in nano range (50 nm). The darker portion in the TEM images shows the inorganic part and greyish part indicated the presence of organic part.

### 3.3 Binary separations

Binary separations of some metal ion pairs, such as  $\text{Cd}^{2+}$ – $\text{Al}^{3+}$ ,  $\text{Cd}^{2+}$ – $\text{Ni}^{2+}$ ,  $\text{Mg}^{2+}$ – $\text{Pb}^{2+}$ ,  $\text{Mg}^{2+}$ – $\text{Zn}^{2+}$ ,  $\text{Cu}^{2+}$ – $\text{Pb}^{2+}$ ,  $\text{Co}^{2+}$ – $\text{Cu}^{2+}$ ,  $\text{Al}^{3+}$ – $\text{Co}^{2+}$  and  $\text{Ni}^{2+}$ – $\text{Zn}^{2+}$  have been achieved onto GT/ZTP nanocomposite column. The elution order of the metal ions depends upon the stability of the metal and eluting ligand. Table 4 and Fig. 6 show the order of elution

and eluents used for binary separations. All the separations are quite sharp and recovery was reproducible and quantitative [37, 38].

### 3.4 Photocatalytic activity

GT/ZTP nanocomposite was investigated for the photocatalytic degradation of MV in solar irradiation. Figure 7a shows that 33.66% MV was adsorbed in dark. Figure 7b

**Table 5** Characteristics of GT/ZTP nanocomposite ion exchange membrane

Membrane	Thickness (mm)	Water content (%)	Porosity	Swelling of % weight of wet membrane
M-1	0.65	5.860	$6.7 \times 10^{-5}$	0.645
M-2	<b>0.49</b>	<b>4.279</b>	<b><math>5.5 \times 10^{-5}</math></b>	<b>0.456</b>
M-3	0.56	7.688	$7.8 \times 10^{-5}$	0.589

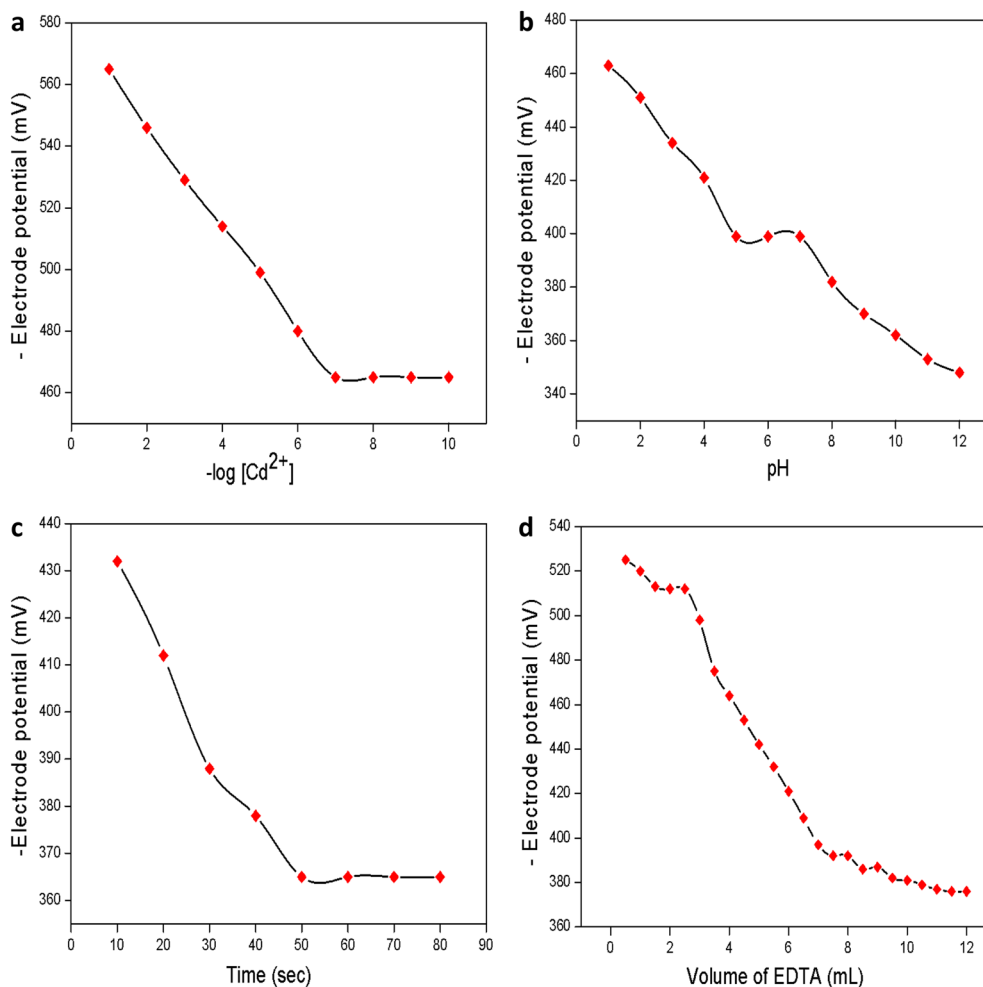
shows the photocatalytic degradation of MV in the presence of sunlight using ZTP and GT/ZTP nanocomposite. ZTP and GT/ZTP nanocomposite degrade about 70.77% and 84.61% of dye within 4 h of solar exposure. Hence, the photocatalytic activity of nanocomposite was found to be higher than inorganic part.

Figure 7c represents the absorption spectra of MV for different irradiation times. It has been found that the adsorption band intensities continuously decreased with irradiation time, which indicated the degradation of dye effectively.

Pseudo-first-order kinetic model for the photodegradation of MV was also examined. MV shows higher value of regression coefficient  $R^2 = 0.998$  and rate constant  $k = 0.02561 \text{ min}^{-1}$  as shown in Fig. 7d.

### 3.5 Potentiometric studies

The membrane M-2 prepared using GT/ZTP nanocomposite with minimum thickness, low water content and porosity



**Fig. 8** a Calibration curve of GT/ZTP nanocomposite ion exchanger membrane electrode in  $\text{Cd}(\text{NO}_3)_2$  solution. b Time response curve. c Effect of pH on potential response at  $1 \times 10^{-2} \text{ mol L}^{-1} \text{ Cd}^{2+}$ . d

Potentiometric titration of Cd(II) ions against EDTA solution with GT/ZTP membrane electrode

was established for ion-selective electrode fabrication as shown in Table 5. Therefore low water content, swelling, porosity and less thickness of membrane indicated small interstices gap and diffusion occurred through the exchanger sites of membrane.

Figure 8a shows the potentiometric response curve of GT/ZTP nanocomposite electrode. The electrode shows a linear response from  $1 \times 10^{-1}$  to  $1 \times 10^{-7}$  mol L<sup>-1</sup> with slope of 18.55 mV. Therefore, the working concentration range of membrane electrode for the detection of Cd(II) was reported upto  $1 \times 10^{-7}$  mol L<sup>-1</sup>.

Figure 8b represents the effect of pH on the potential response of sensor. The results showed that the potential of electrode was constant in the range from 5.0 to 7.0 for Cd(II) ions. The electrode did not give any response below pH 5 and above pH 7 attributed to the metal hydroxide formation [49].

The response time is an essential feature for the analytical applicability of ion-selective electrode. The potential of electrode was examined at different time intervals for cadmium ions as presented in Fig. 8c. The response time for fixed concentration of Cd(II) was found to be 50 s.

The ion selective electrode was employed as an indicator for Cd(NO<sub>3</sub>)<sub>2</sub> solution against EDTA solution as shown in Fig. 8d. It has been found that the potential of electrode decreased by adding EDTA due to complexation of Cd(II) ions with EDTA [50].

## 4 Conclusion

GT/ZTP nanocomposite ion exchanger was prepared using sol-gel method at pH 0–1. GT/ZTP has greater ion exchange capacity as compared to inorganic part. SEM and TEM studies confirmed that the resulting material was in nano range with rough and irregular morphology. Distribution studies confirmed that the nanocomposite was highly selective for Cd(II) ions. Some binary separations of different metal ions were also accomplished onto GT/ZTP column. GT/ZTP nanocomposite degraded 84.61% of MV under solar illumination. GT/ZTP was also exploited for the fabrication of ion-selective membrane electrode to detect the presence of Cd(II) ions.

## Compliance with ethical standards

**Conflict of interest** The authors declare that they have no conflict of interest.

**Publisher's note:** Springer Nature remains neutral with regard to jurisdictional claims in published maps and institutional affiliations.

## References

1. Visa M, Chelaru AM (2014) Hydrothermally modified fly ash for heavy metals and dyes removal in advanced wastewater treatment. *Appl Surf Sci* 303:14–22
2. Saffaj N, Loukili H, Younssi SA, Albizane A, Bouhria M, Persin M, Larbo A (2004) Filtration of solution containing heavy metals and dyes by means of ultrafiltration membranes deposited on support made of Moroccan clay. *Desalination* 168:301–306
3. Liu X, Lee DJ (2014) Thermodynamic parameters for adsorption equilibrium of heavy metals and dyes from wastewaters. *Bioresour Technol* 160:24–31
4. Namasivayam C, Sangeetha D (2006) Recycling of agricultural solid waste, coir pith: removal of anions, heavy metals, organics and dyes from water by adsorption onto ZnCl<sub>2</sub> activated coir pith carbon. *J Hazard Mater* 135:449–52
5. Kadirvelu K, Thamaraiselvi K, Namasivayam C (2001) Removal of heavy metals from industrial wastewaters by adsorption onto activated carbon prepared from an agricultural solid waste. *Bioresour Technol* 76:63–65
6. Pathania D, Sharma G, Thakur R (2015) Pectin@ zirconium (IV) silicophosphate nanocomposite ion exchanger: photo catalysis, heavy metal separation and antibacterial activity. *Chem Eng J* 267:235–244
7. Badruddoza AZ, Shawon ZB, Tay WJ, Hidajat K, Uddin MS (2013) Fe<sub>3</sub>O<sub>4</sub>/cyclodextrin polymer nanocomposites for selective heavy metals removal from industrial wastewater. *Carbohydr Polym* 91:322–332
8. Kim EJ, Lee CS, Chang YY, Chang YS (2013) Hierarchically structured manganese oxide-coated magnetic nanocomposites for the efficient removal of heavy metal ions from aqueous systems. *ACS Appl Mater Interface* 5:9628–9634
9. Sharma G, Pathania D, Naushad M, Kothiyal NC (2014) Fabrication, characterization and antimicrobial activity of polyaniline Th (IV) tungstomolybdophosphate nanocomposite material: efficient removal of toxic metal ions from water. *Chem Eng J* 251:413–421
10. Sarkar S, Chatterjee PK, Cumbal LH, SenGupta AK (2011) Hybrid ion exchanger supported nanocomposites: Sorption and sensing for environmental applications. *Chem Eng J* 166:923–931
11. Bo X, Zhou M, Guo L (2017) Electrochemical sensors and biosensors based on less aggregated graphene. *Biosens Bioelectron* 89:167–186
12. Sharma G, Kumar A, Naushad M, Pathania D, Sillanpaa M (2016) Polyacrylamide@ Zr (IV) vanadophosphate nanocomposite: ion exchange properties, antibacterial activity and photocatalytic behavior. *J Ind Eng Chem* 33:201–208
13. Pathania D, Sharma G, Kumar A, Naushad M, Kalia S, Sharma A, AL-Othman ZA (2015) Combined sorptional-photocatalytic remediation of dyes by polyaniline Zr (IV) selenotungstophosphate nanocomposite. *Toxicol Environ Chem* 97:526–537
14. Pathania D, Thakur M, Mishra AK (2017) Alginate-Zr (IV) phosphate nanocomposite ion exchanger: Binary separation of heavy metals, photocatalysis and antimicrobial activity. *J Alloy Compd* 701:153–162
15. Thakur M, Sharma G, Ahamad T, Ghfar AA, Pathania D, Naushad M (2017) Efficient photocatalytic degradation of toxic dyes from aqueous environment using gelatin-Zr (IV) phosphate nanocomposite and its antimicrobial activity. *Colloids Surf B* 157:456–463

16. Pathania D, Thakur M, Sharma G, Mishra AK (2018) Tin (IV) phosphate/poly (gelatin-cl-alginate) nanocomposite: Photocatalysis and fabrication of potentiometric sensor for Pb (II). *Mater Today Commun* 14:282–293
17. Pathania D, Thakur M, Sharma A, Agarwal S, Gupta VK (2017) Synthesis of lactic acid–Zr (IV) phosphate nanocomposite ion exchanger for green remediation. *Ionics* 23:699–706
18. Pathania D, Thakur M, Puri V, Jasrotia S (2018) Fabrication of electrically conductive membrane electrode of gelatin-tin (IV) phosphate nanocomposite for the detection of cobalt (II) ions. *Adv Powder Technol* 29:915–924
19. Thakur M, Pathania D, Sharma G, Naushad M, Bhatnagar A, Khan MR (2018) Synthesis, characterization and environmental applications of a new bio-composite Gelatin-Zr (IV) phosphate. *J Polym Environ* 26:1415–1424
20. Sharma G, Pathania D, Naushad M (2014) Preparation, characterization and antimicrobial activity of biopolymer based nanocomposite ion exchanger pectin zirconium (IV) selenotungstophosphate: application for removal of toxic metals. *J Ind Eng Chem* 20:4482–4490
21. Yu J, Zhang J, Liu S (2010) Ion-exchange synthesis and enhanced visible-light photoactivity of CuS/ZnS nanocomposite hollow spheres. *J Phys Chem C* 114:13642–13649
22. Sharma G, Thakur B, Naushad M, Ala'a H, Kumar A, Sillanpaa M, Mola GT (2017) Fabrication and characterization of sodium dodecyl sulphate@ ironsilicophosphate nanocomposite: Ion exchange properties and selectivity for binary metal ions. *Mater Chem Phys* 193:129–139
23. Khan A, Asiri AM, Rub MA, Azum N, Khan AA, Khan SB, Rahman MM, Khan I (2013) Synthesis, characterization of silver nanoparticle embedded polyaniline tungstophosphate-nanocomposite cation exchanger and its application for heavy metal selective membrane. *Compos Part B Eng* 45:1486–1492
24. Naushad M, Ahamad T, Sharma G, Ala'a H, Albadarin AB, Alam MM, AL-Othman ZA, Alshehri SM, Ghfar AA (2016) Synthesis and characterization of a new starch/SnO<sub>2</sub> nanocomposite for efficient adsorption of toxic Hg<sup>2+</sup> metal ion. *Chem Eng J* 300:306–316
25. Khan AA, Akhtar T (2008) Preparation, physico-chemical characterization and electrical conductivity measurement studies of an organic–inorganic nanocomposite cation-exchanger: poly-o-toluidine Zr (IV) phosphate. *Electrochim Acta* 53:5540–5548
26. Khan AA, Paquiza L (2011) Analysis of mercury ions in effluents using potentiometric sensor based on nanocomposite cation exchanger polyaniline–zirconium titanium phosphate. *Desalination* 272:278–285
27. Bushra R, Naushad M, Adnan R, AL-Othman ZA, Rafatullah M (2015) Polyaniline supported nanocomposite cation exchanger: Synthesis, characterization and applications for the efficient removal of Pb<sup>2+</sup> ion from aqueous medium. *J Ind Eng Chem* 21:1112–1118
28. Khan AA, Baig U (2012) Electrically conductive membrane of polyaniline–titanium (IV) phosphate cation exchange nanocomposite: applicable for detection of Pb (II) using its ion-selective electrode. *J Ind Eng Chem* 18:1937–1944
29. Khan AA, Baig U, Khalid M (2011) Ammonia vapor sensing properties of polyaniline–titanium (IV) phosphate cation exchange nanocomposite. *J Hazard Mater* 186:2037–2042
30. Nabi SA, Shahadat M, Bushra R, Shalla AH, Azam A (2011) Synthesis and characterization of nano-composite ion-exchanger; its adsorption behavior. *Colloids Surf B Bio* 87:122–128
31. Fernandes FM, Ruiz AI, Darder M, Aranda P, Ruiz-Hitzky E (2009) Gelatin-clay bio-nanocomposites: structural and functional properties as advanced materials. *J Nanosci Nanotechnol* 9:221–229
32. Lee WF, Lee SC (2006) Effect of hydrotalcite on the swelling and mechanical behaviors for the hybrid nanocomposite hydrogels based on gelatin and hydrotalcite. *J Appl Polym Sci* 100:500–507
33. Reddy PR, Varaprasad K, Sadiku R, Ramam K, Reddy GV, Raju KM, Reddy NS (2013) Development of gelatin based inorganic nanocomposite hydrogels for inactivation of bacteria. *J Inorg Organomet Polym Mater* 23:1054–1060
34. Wang K, Nune KC, Misra RD (2016) The functional response of alginate-gelatin-nanocrystalline cellulose injectable hydrogels toward delivery of cells and bioactive molecules. *Acta Biomater* 36:143–151
35. Zhou Z, Liu YG, Liu SB, Liu HY, Zeng GM, Tan XF, Yang CP, Ding Y, Yan ZL, Cai XX (2017) Sorption performance and mechanisms of arsenic (V) removal by magnetic gelatin-modified biochar. *Chem Eng J* 314:223–231
36. Khan MN, Islam JM, Khan MA (2012) Fabrication and characterization of gelatin-based biocompatible porous composite scaffold for bone tissue engineering. *J Biomed Mater Res B* 100:3020–3028
37. Sharma G, Pathania D, Naushad M (2015) Preparation, characterization, and ion exchange behavior of nanocomposite polyaniline zirconium (IV) selenotungstophosphate for the separation of toxic metal ions. *Ionics* 21:1045–1055
38. Pathania D, Sharma G, Naushad M, Kumar A (2014) Synthesis and characterization of a new nanocomposite cation exchanger polyacrylamide Ce (IV) silicophosphate: photocatalytic and antimicrobial applications. *J Ind Eng Chem* 20:3596–3603
39. Khan AA, Baig U (2012) Electrically conductive membrane of polyaniline–titanium (IV) phosphate cation exchange nanocomposite: Applicable for detection of Pb (II) using its ion-selective electrode. *J Ind Eng Chem* 18:1937–1944
40. Khan AA, Habiba U, Khan A (2009) Synthesis and characterization of organic-inorganic nanocomposite poly-o-anisidine Sn (IV) arsenophosphate: its analytical applications as Pb (II) ion-selective membrane electrode. *Int J Anal Chem* 2009 1-10
41. AL-Othman ZA, Alam MM, Naushad M, Bushra R (2015) Electrical conductivity and thermal stability studies on polyaniline Sn (IV) tungstomolybdate nanocomposite cation-exchange material: application as Pb (II) ion-selective membrane electrode. *Int J Electrochem Sci* 10:2663–2684
42. Khan A, Khan AA, Asiri AM, Al-Sehemi AG, Marwani HM (2015) Sol–gel synthesis of poly (o-toluidine)@ Sn (II) silicate/CNT composites for ion selective membrane electrodes. *J Mol Liq* 208:71–77
43. Tripathi BP, Kumar M, Shahi VK (2009) Highly stable proton conducting nanocomposite polymer electrolyte membrane (PEM) prepared by pore modifications: an extremely low methanol permeable PEM. *J Memb Sci* 327:145–154
44. Khan A, Asiri AM, Khan AA, Rub MA, Azum N, Rahman MM, Khan SB, Alamry KA, AbGhani S (2013) Sol–gel synthesis and characterization of conducting polythiophene/tin phosphate nano tetrapod composite cation-exchanger and its application as Hg (II) selective membrane electrode. *J Sol-Gel Sci Technol* 65:160–169
45. Semagne B, Diaz I, Kebede T, Tadesse AM (2016) Synthesis, characterization and analytical application of polyaniline tin (IV) molybdophosphate composite with nanocrystalline domains. *React Funct Polym* 98:17–23
46. Saad M, Tahir H, Khan J, Hameed U, Saud A (2017) Synthesis of polyaniline nanoparticles and their application for the removal of crystal violet dye by ultrasonicated adsorption process based on response surface methodology. *Ultrason Sonochem* 34:600–8
47. Sharma G, Thakur B, Naushad M, Ala'a H, Kumar A, Sillanpaa M, Mola GT (2017) Fabrication and characterization of sodium dodecyl sulphate@ ironsilicophosphate nanocomposite: ion

- exchange properties and selectivity for binary metal ions. *Mater Chem Phys* 193:129–39
48. Nabi SA, Shalla AH (2009) Synthesis, characterization and analytical application of hybrid; acrylamide zirconium (IV) arsenate a cation exchanger, effect of dielectric constant on distribution coefficient of metal ions. *J Hazard Mater* 163:657–664
49. Kaushal S, Badru R, Kumar S, Mittal SK, Singh P (2016) Fabrication of a mercury (II) ion selective electrode based on poly-*o*-toluidine–zirconium phosphoborate. *RSC Adv* 6:3150–3158
50. Kaushal S, Mittal SK, Singh AP, Singh P (2017) Zirconium (IV) phosphoborate-based ion selective membrane electrode for potentiometric determination of Ba (II) ions. *Asian J Chem* 29:375